UPWIND RESIDUAL DISCRETIZATION OF ENHANCED BOUSSINESQ EQUATIONS FOR WAVE PROPAGATION OVER COMPLEX BATHYMETRIES

Mario Ricchiuto and A.G. Filippini

INRIA - Equipe BACCHUS -

Centre de Bordeaux sud-ouest

23 April 2013

Context

Aim: accurately simulate nonlinear and dispersive water waves in near-shore zones.

- the best description: 3D incompressible Navier-Stokes equations
- depth-average approximation and 2D restriction

Models in one-dimension

- Nonlinear Shallow Water equations (NLSW):

$$\begin{cases} \partial_t \eta + \partial_x q = 0 \\ \partial_t q + \partial_x (uq) + gH\partial_x \eta = 0 \end{cases} \tag{1}$$

- Madsen-Sørensen Boussinesq's equations (MS)[1]: back

$$\begin{cases} \partial_t \eta + \partial_x q = 0 \\ \partial_t q - Bh^2 \partial_{x^2 t} q - \frac{1}{3} h \partial_x h \partial_{xt} q + \partial_x (uq) + gH\partial_x \eta + \\ \qquad - \beta g h^3 \partial_{x^3} \eta - 2\beta g h^2 \partial_x h \partial_{x^2} \eta = 0 \end{cases} \tag{2}$$

back

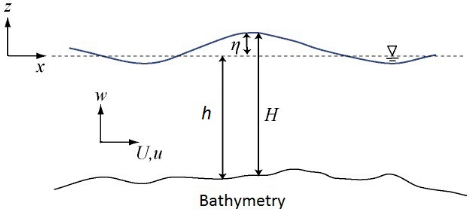

System variables:

- η: free surface water level
- q: mass flux ($q = Hu$)

$\beta = 1/15; \quad B = \beta + \frac{1}{3}$

[1] P. A. Madsen and O. R. Sørensen *Coastal Engineering* 18 1992

Dispersion Analysis

Fourier dispersion analysis, substituting the mode $W = W_0 e^{\nu t + jkx}$, allows to recover the eigenvalue problem $(\nu I + jkA)W = 0$ (being k the wave number and $\nu = \xi + j\omega$). The solution of the characteristic polynomial in its real and imaginary part leads to:

$$\begin{cases} \xi_{SW} = 0 \\ \omega_{SW}^2 = C_0^2 k^2 \end{cases} \qquad \begin{cases} \xi_{MS} = 0 \\ \omega_{MS}^2 = C_0^2 k^2 \dfrac{1 + \beta\mu^2}{1 + B\mu^2} \end{cases} \tag{3}$$

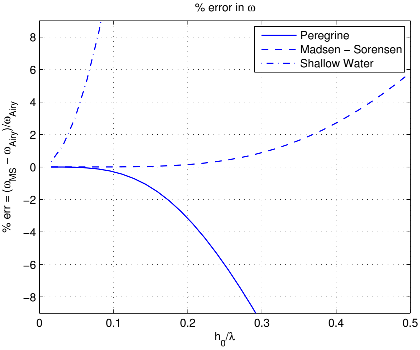

The error is computed w.r.t C_{Airy}:

$$\begin{cases} \xi_{\text{Airy}} = 0 \\ \omega_{\text{Airy}}^2 = C_0^2 k^2 \dfrac{\tanh(\mu)}{\mu} \end{cases} \tag{4}$$

being:

- C_0: SW wave celerity ($C_0^2 = gh_0$)
- $\mu = kh_0$

Models in one-dimension

- The MS model allows a better prediction of wave propagation and shoaling in the near shore region $h_0/\lambda \to 0.5$
- However the NLSW are a
  1. quite good in run up and backwash regions (flooding and drying)
  2. **a good model for wave breaking** the energy dissipation of a NLSW shock being an excellent approximation of the energy transformation in a roller[2]

Complete description of the near-shore dynamics by coupling MS (Boussinesq) with NLSW to handle breaking and dry fronts

[2] P. Bonneton *Ocean Engineering* 67 2007, P. Bonneton et al. *JCP* 230 2011)

Objectives

The numerical scheme must satisfy the following requirements:

- accuracy, in particular low dispersion error
- efficiency : compact stencil, unstructured adaptive meshes
- Ability to handle both Boussinesq (roughly parabolic) and NLSW equations (hyperbolic !)

Objectives

As a first step toward the construction a full unstructured near shore model

Investigate the applicability for the solution of the MS equations of **upwind stabilized** finite elements and residual based discretizations having shown excellent results for the NLSW model[3]

[3] G. Hauke *CMAME* 1-4 1998, M.Ricchiuto, R. Abgrall and H. Deconinck *JCP* 222 2007

P^1 Finite Element Approach

- We consider a tasselation of the domain Ω in non-overlapping elements;
- Unknowns are stored at nodes: $\{\eta_i(t)\}_{i\geq 1}$ and $\{q_i(t)\}_{i\geq 1}$;
- P^1 piecewise linear continuous approximation

$$\begin{aligned} \eta_h(t,x) &= \sum_{i\geq 1} \eta_i(t)\varphi_i(x) = \sum_K \sum_{j\in K} \eta_j(t)\varphi_j(x) \\ q_h(t,x) &= \sum_{i\geq 1} q_i(t)\varphi_i(x) = \sum_K \sum_{j\in K} q_j(t)\varphi_j(x) \end{aligned} \tag{5}$$

- φ_i are standard continuous piecewise linear finite element basis functions;

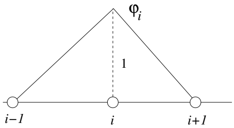

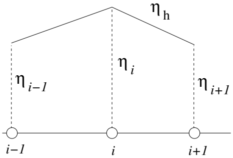

Continuous Galerkin approximation (cG)[4]

$$\int_{\Omega_h} \varphi_i \partial_t \eta_h - \int_{\Omega_h} q_h \, \partial_x \varphi_i = 0$$

$$\int_{\Omega_h} \varphi_i \partial_t q_h + \int_{\Omega_h} B \partial_{xt} q_h \partial_x (h^2 \varphi_i) - \int_{\Omega_h} \frac{1}{3} \varphi_i h \partial_x h \partial_{xt} q_h - \int_{\Omega_h} (uq)_h \partial_x \varphi_i - \int_{\Omega_h} g \frac{H_h^2}{2} \partial_x \varphi_i$$
$$- \int_{\Omega_h} \varphi_i g H_h \partial_x h - \int_{\Omega_h} \varphi_i \beta g h^3 \partial_x w_h^\eta - \int_{\Omega_h} \varphi_i 2 \beta g h^2 \partial_x h \, w_h^\eta = 0$$

$$\int_{\Omega_h} \varphi_i w_h^\eta + \int_{\Omega_h} \partial_x \eta_h \partial_x \varphi_i = 0$$

4 M.A. Walkley and M. Berzinz *IJNMF* 39 2002, C. Eskilsson and S. Sherwin *JCP* 210 2006

Continuous Galerkin approximation (cG)[5]

$$\int_{\Omega_\mathrm{h}} \varphi_i \partial_t \eta_\mathrm{h} - \int_{\Omega_\mathrm{h}} q_\mathrm{h}\, \partial_x \varphi_i = 0$$

$$\int_{\Omega_\mathrm{h}} \varphi_i \partial_t q_\mathrm{h} + \int_{\Omega_\mathrm{h}} B \partial_{xt} q_\mathrm{h} \partial_x (h^2 \varphi_i) - \int_{\Omega_\mathrm{h}} \frac{1}{3} \varphi_i h \partial_x h \partial_{xt} q_\mathrm{h} - \int_{\Omega_\mathrm{h}} (uq)_\mathrm{h} \partial_x \varphi_i - \int_{\Omega_\mathrm{h}} g \frac{H_\mathrm{h}^2}{2} \partial_x \varphi_i$$
$$- \int_{\Omega_\mathrm{h}} \varphi_i g H_\mathrm{h} \partial_x h - \int_{\Omega_\mathrm{h}} \varphi_i \beta g h^3 \partial_x w_\mathrm{h}^\eta - \int_{\Omega_\mathrm{h}} \varphi_i 2\beta g h^2 \partial_x h\, w_\mathrm{h}^\eta = 0$$

$$\int_{\Omega_\mathrm{h}} \varphi_i w_\mathrm{h}^\eta + \int_{\Omega_\mathrm{h}} \partial_x \eta_\mathrm{h} \partial_x \varphi_i = 0$$

[5] M.A. Walkley and M. Berzinz *IJNMF* 39 2002, C. Eskilsson and S. Sherwin *JCP* 210 2006

Central Residual Distribution Scheme (cRD) [6]

Given the initial values of the solution in the nodes of the mesh:

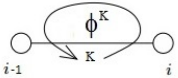

1. residual Φ^K is computed on the initial nodal values $\forall$ element K of the mesh: back

$$\Phi^K = \begin{bmatrix} \Phi^K_\eta & \Phi^K_q \end{bmatrix}^T$$

$$\Phi^K_\eta = \int_K \left(\partial_t \eta_{h|_K} + \partial_x q_{h|_K} \right) dx$$

$$\Phi^K_q = \int_K \Bigg(\partial_t q_{h|_K} - Bh^2 \partial_{x^2 t} q_{h|_K} - \frac{1}{3} h \partial_x h \partial_{xt} q_{h|_K} + \partial_x (uq)_{h|_K} + \\ + gH \partial_x \eta_{h|_K} - \beta g h^3 \partial_{x^3} \eta_{h|_K} - 2\beta g h^2 \partial_x h \partial_{x^2} \eta_{h|_K} \Bigg) dx$$

[6] M.Ricchiuto, R. Abgrall and H.Deconink *JCP* 222 2007, M. Ricchiuto and A. Bollerman *JCP* 228 2009

Central Residual Distribution Scheme (cRD) [6]

Given the initial values of the solution in the nodes of the mesh:

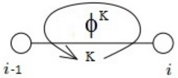

1. residual Φ^K is computed on the initial nodal values $\forall$ element K of the mesh: back

$$\Phi^K = \begin{bmatrix} \Phi_\eta^K & \Phi_q^K \end{bmatrix}^T$$

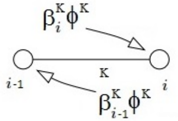

2. the residual is distributed between the nodes which belong to K by means of the weighting coefficient β_i^K:

$$\sum_i \Phi_i^K = \Phi^K$$
$$\Phi_i^K = \beta_i^K \Phi^K$$

[6] M.Ricchiuto, R. Abgrall and H.Deconink *JCP* 222 2007, M. Ricchiuto and A. Bollerman *JCP* 228 2009

Central Residual Distribution Scheme (cRD) [6]

Given the initial values of the solution in the nodes of the mesh:

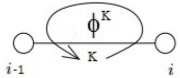

1. residual Φ^K is computed on the initial nodal values $\forall$ element K of the mesh: back

$$\Phi^K = \begin{bmatrix}\Phi^K_\eta & \Phi^K_q\end{bmatrix}^T$$

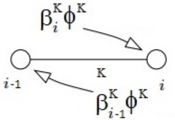

2. the residual is distributed between the nodes which belong to K by means of the weighting coefficient β^K_i:

$$\sum_i \Phi^K_i = \Phi^K$$
$$\Phi^K_i = \beta^K_i \Phi^K$$

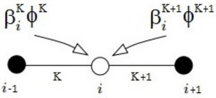

3. $\forall$ nodes $i \in \Omega_h$ nodal values are computed assembling residual fluxes from the adjacent elements:

$$\sum_{K \in K_i} \Phi^K_i = \frac{1}{2}\Phi^K + \frac{1}{2}\Phi^{K+1} = 0 \qquad (6)$$

[6] M.Ricchiuto, R. Abgrall and H.Deconink *JCP* 222 2007, M. Ricchiuto and A. Bollerman *JCP* 228 2009

Auxiliary Variables

Higher order derivatives are poorly represented for C^0 continuous FE space (actually locally null in the P^1 case):

cG: 3^{rd} order derivative $\left(\beta g h^3 \partial_{x^3} \eta\right)$ go

cRD: 2^{nd} order and third order derivatives $\left(B h^2 \partial_{x^2 t} q;\ 2\beta g h^2 \partial_x h \partial_{x^2} \eta\right)$

- New *auxiliary variables* $w_\eta,\ w_q$.
- Extra algebraic equation for each variable introduced:
  $\Rightarrow\ w_\eta = \partial_{x^2}\eta;\ w_q = \partial_x q$

Auxiliary Variables

Approximation and cost: L^2 projection with mass lumping[7]

$$\Delta x \; w_{\mathrm{h}}^{\eta} + \int_{\Omega_{\mathrm{h}}} \partial_x \eta_{\mathrm{h}} \partial_x \varphi_i = 0$$

$$\Delta x \; w_{\mathrm{h}}^{q} + \int_{\Omega_{\mathrm{h}}} q \, \partial_x \varphi_i = 0$$

cost of a Green-Gauss reconstruction for each new variable ..

[7] M.A. Walkley and M. Berzinz *IJNMF* 39 2002

Stabilized Upwind Schemes (SUPG and uRD)

Schemes **cG** and **cRD** are centered approximations not well suited for the discretization of the Shallow Water limit for which some form of upwinding is necessary to stabilize the system.

Stabilized Upwind Schemes (SUPG and uRD)

Streamline Upwind Petrov-Galerkin stabilization[8] :

$$\mathcal{R}_i(\eta_h, q_h) + \sum_{\mathsf{K}\in\Omega_h} A^{\mathsf{K}} \partial_x \varphi_i^{\mathsf{K}} \tau_{\mathsf{K}} \Phi^{\mathsf{K}} = 0 \tag{7}$$

A^{K} linearized NLSW flux Jacobian, and τ_{K} is the SUPG stabilization parameter:

$$\tau_{\mathsf{K}} = \frac{1}{\sum_{j\in\mathsf{K}} |\partial_x \varphi_j^K|} |A^{\mathsf{K}}|^{-1}$$

[8] T.J.R Hughes, G. Scovazzi and T. Tezduyar, *J.Sci.Comp.* 43 2010

Stabilized Upwind Schemes (SUPG and uRD)

The final form:

$$\mathcal{R}_i(\eta_h, q_h) + \sum_{\mathrm{K}\in\Omega_h} \mathrm{sign}(\partial_x \varphi_i^{\mathrm{K}}) \frac{\mathrm{sign}(A^{\mathrm{K}})}{2} \Phi^{\mathrm{K}} = 0 \tag{8}$$

$\mathcal{R}_i$ is the centred part of the scheme: if $\mathcal{R}_i^{cG} \longrightarrow$ **SUPG** scheme;

if $\mathcal{R}_i^{cRD} \longrightarrow$ **uRD** scheme.

Upwinding on the NLSW characteristics. The URD : upwind distribution of MS integrated residual on NLSW charactersitics

Truncation Error

	FD2	FD4	cG	cRD	SUPG	URD
TE_η	Δx^2	Δx^4	$\boldsymbol{\Delta x^4}$	Δx^2	$\boldsymbol{\Delta x^3}$	Δx^2
TE_u	Δx^2	Δx^4	Δx^2	Δx^2	Δx^2	Δx^2

Dispersion Error

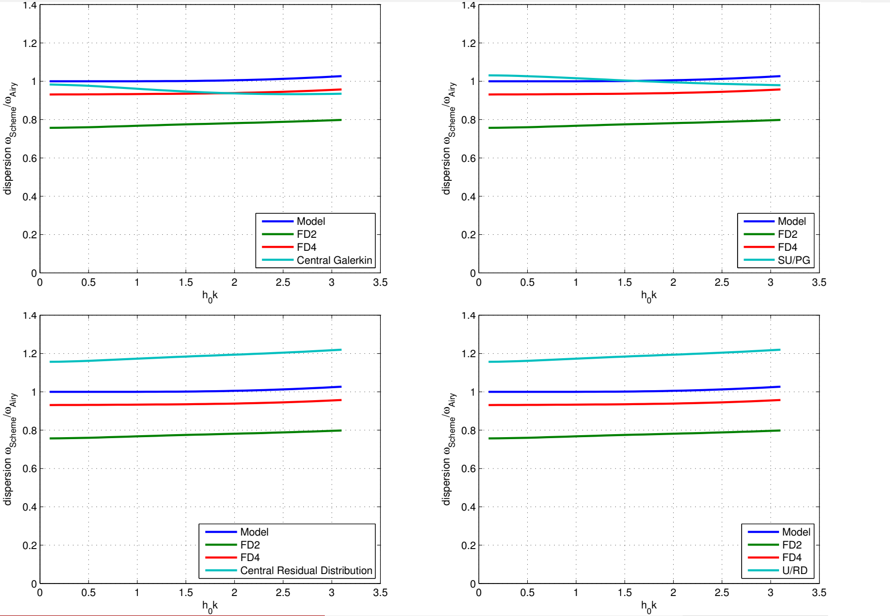

Dispersion Error

cRD and **URD** schemes provide phase errors comparable to those of the **FD2** scheme, giving nearly identical results.
cG and **SUPG** are at least as good if not better than the **FD4** scheme.

SUPG scheme our best candidate for an upwind discretization of the MS equations

Numerical solution

Newton Iterations

Crank-Nicolson (**CN**) in time (simple, A-stable, non dissipative)
Newton iteration method with frozen Jacobian ◂ back

1. Set $W_0 = (\eta_0^{n+1},\, q_0^{n+1})^T = (\eta^n\, q^n)^T$;
2. Evaluate the *frozen* Jacobian matrix : $\mathcal{M} = \dfrac{\partial F}{\partial W_h}(W_h = W_0|\eta_h^n,\, q_h^n)$
3. Compute a LU factorization of $\mathcal{M}$;
4. for $\mathrm{k} = 1,\, \mathrm{k}_{\max}$ do:
    1. Evaluate $F(W_{k-1}|\eta_h^n,\, q_h^n)$;
    2. If $\|F\| \leq \epsilon$ set $\mathrm{k} = \mathrm{k}_{\max}$ and exit, else evaluate $W_k = W_{k-1} - \mathcal{M}^{-1} F(W_{k-1}|\eta_h^n,\, q_h^n)$;
5. Set $W_h = W_{\mathrm{k}_{\max}}$.

Propagation Test

Propagation of a 0.2 m amplitude soliton in still water of constant depth 1 m.

SUPG results on $\Delta x = 0.1$m mesh

- good amplitude and shape conservation;
- no sensible dispersion effect during the propagation;
- the information propagates at the physically correct speed.

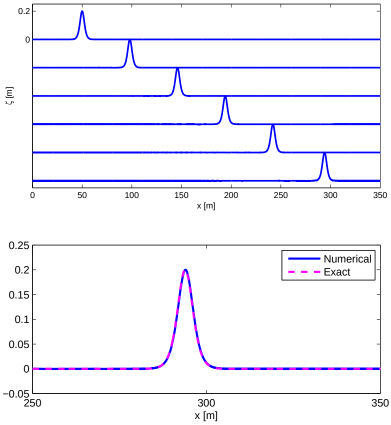

Grid Convergence

To isolate the error in space time step has been set to:

$$\Delta t = 100 \frac{\Delta x^3}{C}$$

with C the celerity of the solitary. Error computed after a 100m displacement

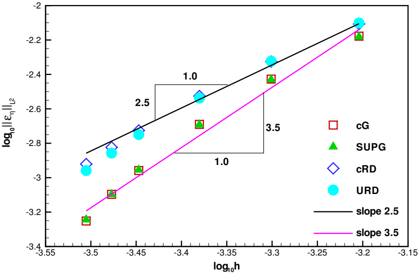

The convergence rates of the L^2 norm of the error in the amplitude η show:

- high accuracy of **cG** and **SUPG** (between 3 and 4);
- effect of stabilization barely visible (surprising)

Head-on Collision of Two Solitary Waves

Propagation of two 0.2 m amplitude converging solitons in still water of constant depth 1 m

The soliton property of emerging unchanged from the collisions with other solitons is well captured, except for a small phase shift and amplitude over-estimation.

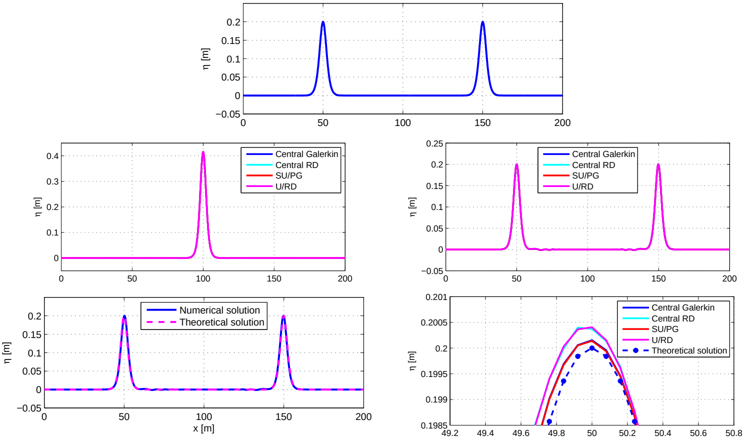

Periodic Wave Propagation over a Submerged Bar (1)

Test Description: $a = 0.01$ m; $T = 2.02$ s; $\Delta x = 0.04$ m; $\Delta t = 0.0323$ s

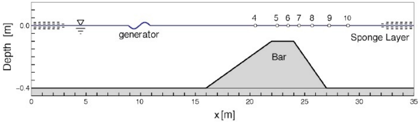

- ∘ experimental data;
- — **cG** scheme;
- — **SUPG** scheme;
- — **uRD** scheme.

A *phase calibration* has been necessary to compare computed and measured signals minimizing the error w.r.t. the data of gauge 4.

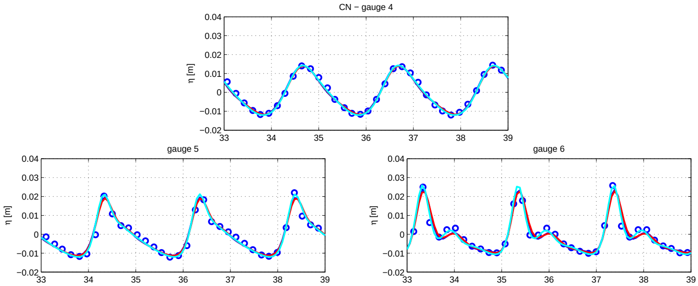

Periodic Wave Propagation over a Submerged Bar (2)

Schemes Comparison

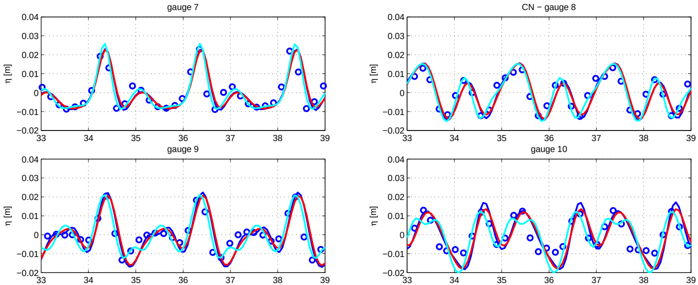

The results have good agreement, showing only a weak phase shift despite the strong nonlinearity.

As the waves pass the bar higher harmonics arise from the primary longer wave.

The **SUPG** scheme appears to be less sensible to this kind of problems.

Enhanced Boussinesq equations in 2D

Madsen-Sørensen system of 2D Boussinesq's equations (in the form [7]): go

$$
\begin{cases}
\partial_t \eta + \nabla \cdot \vec{q} = 0 \\
\partial_t q + \nabla \cdot (\vec{u} \otimes \vec{q}) + gH\nabla\eta + \vec{\psi} = 0
\end{cases}
\tag{9}
$$

the dispersive terms $\vec{\psi} \equiv (\psi_x, \psi_y)$ are written as:

$$
\begin{cases}
\psi_x = -Bh^2 \partial_{tx} \nabla \cdot \vec{q} - \frac{1}{6} h \partial_x h \partial_t \left(\nabla \cdot \vec{q} + \partial_x q_x \right) - \frac{1}{6} h \partial_y h \partial_{tx} q_y - \beta g h^2 \partial_x w^\eta \\
\psi_y = -Bh^2 \partial_{ty} \nabla \cdot \vec{q} - \frac{1}{6} h \partial_y h \partial_t \left(\nabla \cdot \vec{q} + \partial_y q_y \right) - \frac{1}{6} h \partial_x h \partial_{ty} q_x - \beta g h^2 \partial_y w^\eta \\
w^\eta = \nabla \cdot (h \nabla \eta)
\end{cases}
\tag{10}
$$

- Auxiliary variables : w^η, $w^{q_x} = \nabla q_x$, and $w^{q_y} = \nabla q_y$
- Numerical implementation of SUPG identical to the 1D case

[7] H.A. Schaffer and P.A. Madsen Coastal Engineering 26 1995

Wave diffraction over a semi-circular shoal (1)

Test Description: waves period $T = 2$s; amplitude $A = 0.0075$m;
computational domain $[-10, 36]m \times [0, 6.096]m$.

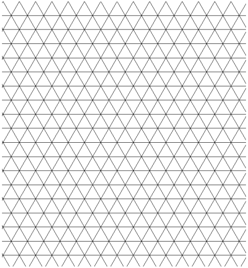

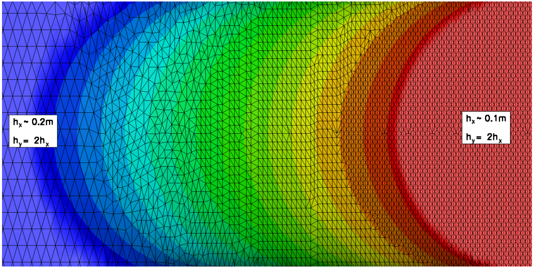

LEFT: uniform grid with mesh size in the x direction uniform and equal to $h_x = 0.1$m. (≈64k elements)

RIGHT: unstructured triangulation with $h_x \approx 0.2$m and progressively reduced when approaching the shoal to reach the value o $h_x \approx 0.1$m. (≈ 31k elements)

For both grids in the y direction $h_y = 2h_x$.

Computations have been run for 100s with $\Delta t \approx 0.03$.

Wave diffraction over a semi-circular shoal (2)

Numerical results and comparison w.r.t. experimental data

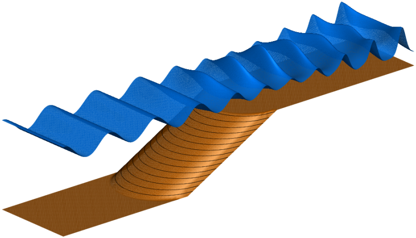

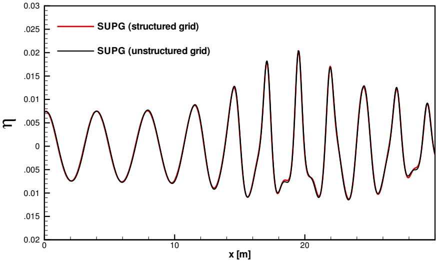

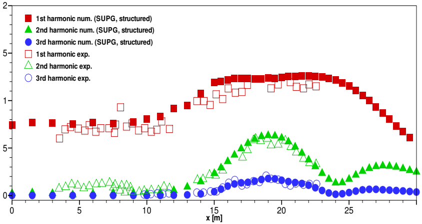

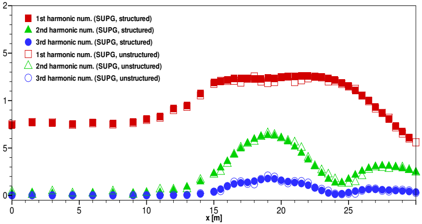

Wave diffraction over an elliptic shoal (1)

Test Description: computational domain $[-10, 10]m \times [-17, 15]m$;
unstructed mesh refined from $h_y \approx 0.1$ to $h_y \approx 0.05$ along y and with $h_x = 2h_y$

Studying the refraction and diffraction of monochromatic waves over a complex bathymetry.

Computations have been run until time $t = 50$s with $\Delta t \approx 0.02$s.

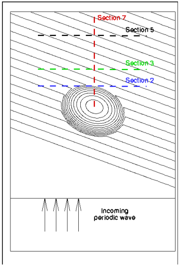

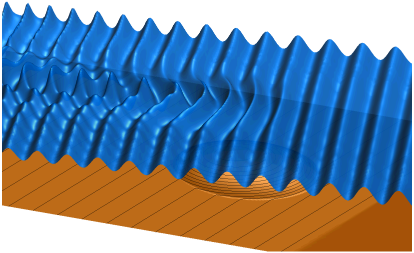

Wave diffraction over an elliptic shoal (2)

Comparison with experimental data

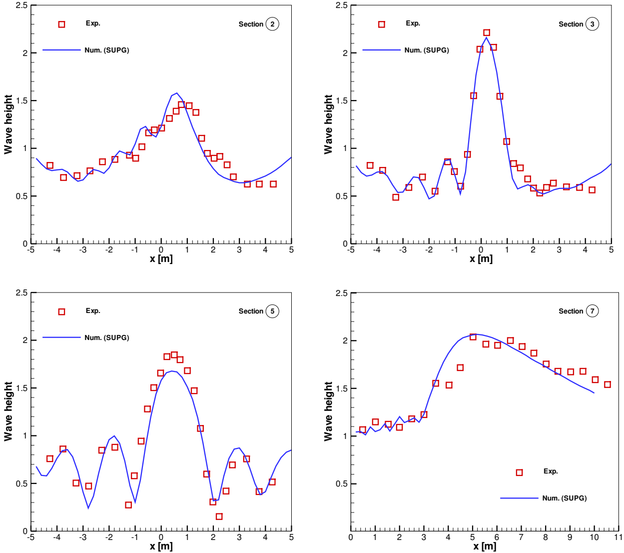

Conclusions

- First step toward a full continuous FEM unstructured model for near-shore wave propagation coupling an enhanced Boussinesq model and Shallow Water equations
- Study of different upwind stabilized residual schemes : upwind bias of full residual along the NLSW characteristics
- Theoretical error and numerical validation
- Very promising features of the SUPG scheme

Work in progress

- Wave breaking by reverting to NLSW

(wave breaking over a shelf)

- Improving numerics :
  - FEM basis (spectral, nurbs, p-adaptive)
  - time dependent mesh adaptation
- Fully nonlinear models such as *Green-Naghdi* eq.s[8]

[8] Bonneton et al *JCP* 230 2011